Check for updates

Wiley
International Journal of Energy Research
Volume 2024, Article ID 3249514, 11 pages
https://doi.org/10.1155/er/3249514

WILEY

Research Article

Blue Hydrogen Production Through Partial Oxidation: A Techno-Economic and Life Cycle Assessment

Navid Khallaghi,[1] **Shamsoddin Ghiami**,[2] **Harish Jeswani**,[3] **Seyed Ali Nabavi**,[1] **and Edward J. Anthony**[1]

[1]*Centre for Climate and Environmental Protection, Cranfield University, MK43 0AL, Bedford, Bedfordshire, UK*
[2]*Department of Mechanical Engineering, School of Engineering and Built Environment, Edinburgh Napier University, Edinburgh, UK*
[3]*Department of Chemical Engineering, University of Manchester, M13 9PL, Manchester, UK*

Correspondence should be addressed to Navid Khallaghi; n.khallaghi@cranfield.ac.uk

Received 10 July 2024; Accepted 19 October 2024

Academic Editor: Semen Klyamkin

Copyright © 2024 Navid Khallaghi et al. This is an open access article distributed under the Creative Commons Attribution License, which permits unrestricted use, distribution, and reproduction in any medium, provided the original work is properly cited.

Partial oxidation (POx) as a hydrogen production method has not received comprehensive exploration as the resulting syngas has a relatively low H_2/CO ratio compared to established techniques like steam methane reforming (SMR). As a result, this study aims to comprehensively investigate the feasibility of a low-carbon hydrogen production process using POx from both technical-economic and environmental standpoints. To achieve this, the Aspen Plus® software is employed to model a hydrogen production plant with carbon capture integration, referred to as POx-CCS (carbon capture and storage). The research reveals that the overall energy efficiency of the POx-CCS process is around 73%. Moreover, the economic evaluation indicates that the levelised cost of hydrogen (LCOH) is €1.8/ kg_{H2}, given a fuel price of €5.7 per GJ. This cost competitiveness positions POx-CCS in line with conventional hydrogen production methods. From an environmental perspective, the impact of climate change on hydrogen production through the POx-CCS process is assessed to be 1.1 kg CO_2 eq./kg_{H2}. This impact is reduced by 69% compared to SMR with CCS.

Keywords: carbon capture; cost of CO_2 capture; greenhouse gas emissions; partial oxidation

1. Introduction

Hydrogen can serve as an alternative to fossil fuels due to its high energy content and carbon-free nature [1]. Worldwide hydrogen use can be allocated to four sectors: ammonia production (50%), refinery applications (22%), methanol production (14%) and reduction processes, including ferrous metallurgy and steelmaking (7%) [2–6]. Although multiple green hydrogen production methods have been explored, fossil fuels are still responsible for over 95% of hydrogen production [7, 8]. Therefore, decarbonising the gas network with low-carbon hydrogen can improve the economic life of the existing gas infrastructure. In addition, it has financial and environmental benefits by delaying the commissioning costs and reducing and avoiding emissions associated with the construction of new infrastructure [9]. Moreover, utilising blue hydrogen will pave the way for green hydrogen production in the longer term, including new distribution systems opening up for different hydrogen applications.

Low-carbon hydrogen production is crucial in accelerating the efforts to achieve decarbonising, owing to its potential for almost emission-free combustion, substantial energy density, versatile applicability and operational efficiency [10]. The drive for low-carbon hydrogen production revolves around two principal routes: deriving 'blue hydrogen' from fossil fuel sources, notably natural gas (NG) with carbon capture and adopting electrolysis powered by low-carbon electricity sources [11]. It is imperative to recognise that hydrogen production via steam methane reforming (SMR), as the primary means of hydrogen generation [12, 13], inherently results in CO_2 emissions ranging from 7.5 to 12 tonnes of CO_2 per ton of hydrogen produced [14]. Several research groups have undertaken comprehensive techno-economic evaluations concerning the feasibility of blue-hydrogen generation

through SMR coupled with carbon capture and storage (CCS) methodologies. Gaudernack and Lynum [15] studied the economic aspects of gas steam reforming in the presence/absence of CO_2 capture. They reported a CAPEX of 25.54 €/Nm^3_{H2} and 14.11 €/Nm^3_{H2} and the OPEX of 4.11 €/Nm^3_{H2} and 3.51 €/Nm^3_{H2}, respectively. Gangadharan et al. [16] evaluated the enviro-economic impact of SMR and reported that its CAPEX is approximately 15.6 M€, the OPEX is 4296€/h and the potential environmental impact (PEI) is 2.84E + 4 PEI/h. Salkuyeh et al. [17] investigated H_2 production without/with CCS. They revealed that CCS implementation results in a higher CAPEX of 682.4 M€ in comparison with the case without CCS (197.9 M€), and, respectively, results in the H_2 production cost of 1.77 €/kg_{H2} and 0.89 €/kg_{H2}. Moreover, the life cycle assessment (LCA) results illustrated that the SMR without CCS has the highest global warming potential (GWP), equivalent to 11.5 kg CO_2 eq./kg H_2. Roussanaly et al. [18] utilised HYSYS v9.0 and the iCCS CO_2 value chain tool to simulate an SMR system with 450 t_{H2}/day capacity in the presence and absence of CCS. They demonstrated that a non-retrofitted SMR system's net power output deteriorated by 47.5% due to CCS power requirement with the respective H_2 production costs of 0.18 €/Nm^3_{H2} and 0.12 €/Nm^3_{H2}. Moreover, the cost of CO_2 avoidance is shown to be 38.23 €/$t_{CO2,avoided}$.

The partial oxidation (POx) approach stands out as a method for producing synthesis gas [19], as it is well known for its simplicity, cost-effectiveness, extended operational lifespan, compact physical footprint, rapid response capabilities and streamlined start-up protocols. However, the practical application of POx necessitates incorporating an air separation unit (ASU), thereby introducing an escalated demand for initial investments and capital expenditures. Furthermore, should the ASU draw power from non-renewable electricity sources, the attendant concern of associated carbon dioxide emissions becomes significant [20]. POx can be classified into two distinct categories: catalytic POx, carried out at approximately 700−1000°C and non-catalytic POx, which operates across a temperature range of 1200−1500°C [21, 22]. The non-catalytic iteration of POx finds particular utility in hydrogen generation from heavy hydrocarbons that show constrained reactivity with conventional catalysts. In cases where coal is employed as the primary feedstock, this process is known as gasification [23]. Several studies have been conducted on POx of different fuels. Wang et al. [24] demonstrated the enhanced performance of a composite Ni-Co/Al_2O_3-TiO_2 catalyst for hydrogen production from propane POx, exhibiting increased hydrogen and carbon monoxide selectivities along with reduced carbon dioxide and methane selectivities. This resulted in improved stability and reduced deactivation compared to a commercial catalyst. To enhance the POx of methanol for H_2 production, three Ni-Cu/Al_2O_3 catalysts with varying Ni weight percentages (10, 20 and 30 wt%) were synthesised [25]. Here, incorporating Ni into a copper catalyst effectively boosts its activity. Notably, the optimal conditions for H_2 yield were observed at $O_2/C = 0.5$, preheating temperature = 150°C, and Ni wt% = 10, resulting in the highest yield of 2 mol_{H2}/mol_{CH3OH}. Levikhin and Boryaev [26] designed a high-temperature reactor (HTR) for producing hydrogen-containing gas through non-catalytic hydrocarbon oxidation. Their work covers the physical model, structural aspects and design principles of HTRs and introduces calculated ratios for evaluating HTR dimensions during the preliminary design, accounting for component types and desired hydrogen gas output. Their experimental results indicated that for diesel fuel/oxygen, hydrogen concentration at the outlet is 41–43 vol% with a H_2/CO ratio of around 0.9. However, for methane/oxygen, hydrogen concentration is 54–57 vol% with a H_2/CO ratio of about 2.1.

However, to the authors' best knowledge, despite extensive research on hydrogen production methods, there is a noticeable lack of publications thoroughly evaluating NG POx from both techno-economic and environmental perspectives. Hence, this research addresses this gap by demonstrating the feasibility of hydrogen production with NG non-catalytic POx integrated with downstream CO_2 absorption. A stand-alone process for a hydrogen production system has been proposed and developed at Aspen Plus. Methyl diethanolamine (MDEA) is considered in this research as it is remarkably more stable and has a lower regeneration energy requirement than other amines. Then, the results obtained from the thermodynamic performance are used for an economic feasibility evaluation. Finally, the proposed cycle's techno-economic analysis is performed using capital cost, levelised cost of hydrogen (LCOH) production and cost of CO_2 capture. Moreover, a LCA is conducted to highlight its environmental performance.

2. Process Description and Model Development

2.1. Process Description. Figure 1 illustrates the suggested hydrogen production process. Here, pressurised NG is completely converted to syngas (mainly comprised of CO, H_2, CO_2, and H_2O) in the reactor in the presence of a substoichiometric quantity of high-purity oxygen from the ASU at 20 bars. The generated syngas is then used for power generation and hydrogen production. A portion of the syngas enters a two-stage water gas shift (WGS) reactor after being depressurised by 3 bars through an expander. The first and second stages of the WGS reaction occur at 488 and 280°C, respectively, with an intermediate heat exchanger. The mixture obtained is then sent to the absorber after condensation at 40°C. The syngas enters the bottom of the absorption column, while the lean MDEA enters from the top. As a result, the CO_2-rich solvent and H_2-enriched stream leave the column from the bottom and top of the absorber, respectively. High-purity hydrogen is obtained after H_2-enriched syngas enters the pressure swing adsorption (PSA) unit with 95% recovery [27]. It is worth mentioning that the PSA tailgas is vented to the atmosphere. Next, the CO_2-rich solvent is pumped into the stripper. After cooling the lean solvent in the intermediate heat exchanger, the lean solvent is sent back to the absorber at a lower pressure in the valve. The CO_2 stream from the stripper is then dehumidified in the condenser, and the gaseous CO_2 exits to the compression conditioning unit for transportation. The current practice for CO_2 transportation is to maintain the pressure above the critical pressure (73.8 bar) due to its high

ijer, 2024, 1, Downloaded from https://onlinelibrary.wiley.com/doi/10.1155/er/3249514 by Cranfield University Kings, Wiley Online Library on [21/01/2025]. See the Terms and Conditions (https://onlinelibrary.wiley.com/terms-and-conditions) on Wiley Online Library for rules of use; OA articles are governed by the applicable Creative Commons License

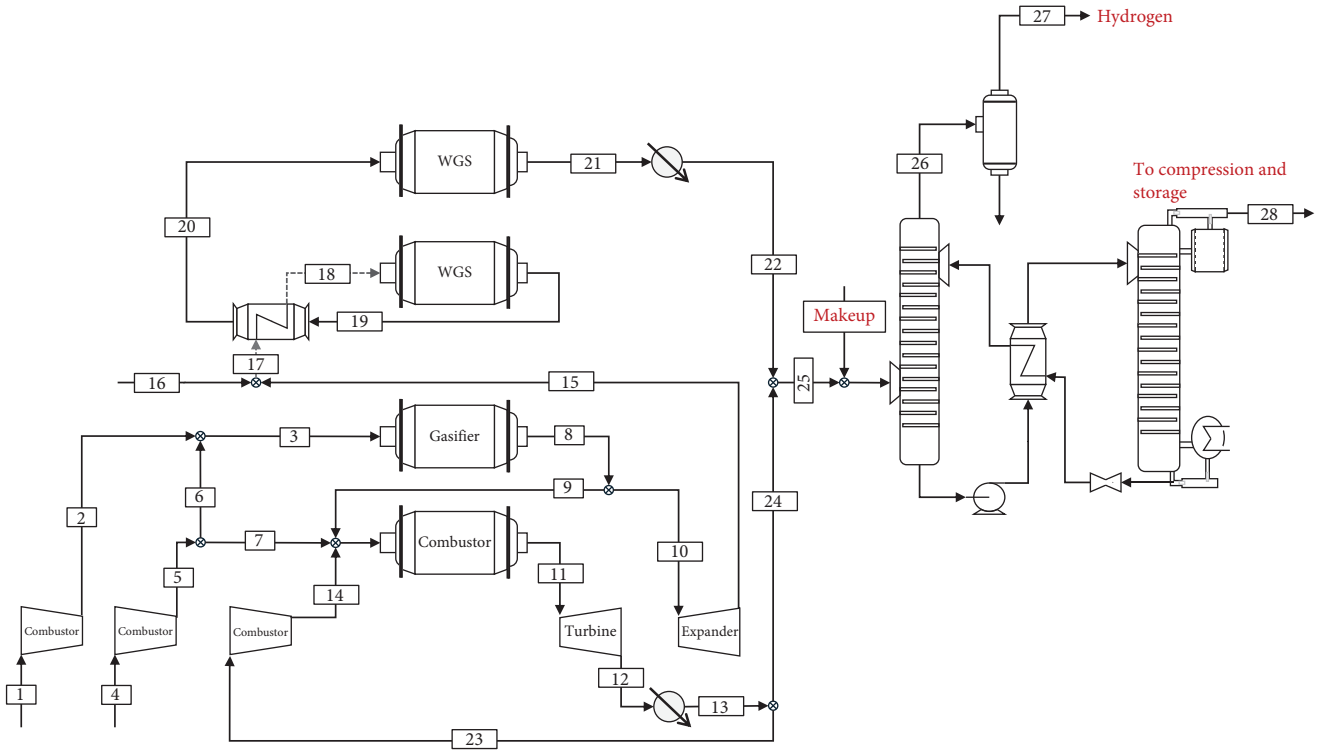

FIGURE 1: Schematic of POx-CCS process. CCS, carbon capture and storage; POx, partial oxidation.

density and low viscosity. To overcome the pressure drop within the transportation pipeline, it is proposed to pressurise CO_2 to well above the critical pressure point (110 bar). For this reason, multistage compressors are utilised to increase the pressure (to 78 bar), and a cooler decreases the temperature (to 25°C) to liquefy the CO_2 stream [28].

Using this approach, oxy-combustion is employed to treat the remaining syngas, high-purity oxygen (95%) and exhaust gas recirculation (mainly CO_2) is used as a temperature moderator. The syngas flow rate used in the power section is adjusted by a splitter compensating for the power consumption of the entire system. This avoids excess power generation from the system to obtain a higher H_2 production rate. After expansion in the turbine, the flue gas is cooled down for condensation. It is then partially recycled back to the combustor to lower the combustion temperature, and the rest is mixed with the H_2-enriched gas entering the MDEA carbon capture unit.

2.2. Model Development. In this study, the process is being simulated in Aspen Plus. The ELECNRTL equation of state is used to simulate the MDEA carbon capture unit, while the Peng–Robinson property model is used for the other parts of the simulation. Moreover, the equilibrium calculation is used to simulate the absorber and stripper columns. The PSA unit is modelled with a simple separator in Aspen Plus with a 95% recovery. Table 1 summarises the parameters used for other components.

The MDEA carbon capture plant was validated by Khallaghi et al. [29], whose results were in agreement with those presented by Romano et al. [30]. For this study, NG is the feedstock, and its properties for gasification are represented in Table 2.

Furthermore, assumptions are made to simulate the POx system, presented in Table 3.

TABLE 1: Aspen plus components used in the process modelling.

Unit	Aspen Plus ID	Description
Condenser	Flash2	Pressure change = 0, duty = 0
Cooler	Heater	—
Heat exchanger(s)	HeatX, MHeatX	—
Combustor	RGibbs	—
Turbine, compressor	Compr, MCompr	—
Expander	Compr	—
Absorber	RadFrac	15 stages, standard convergence
Regenerator	RadFrac	20 stages, partial vapour condenser, standard convergence, reflux ratio = 0.6 mol, boil up ratio = 0.1 mole
WGS	RGibbs	—
Pump	Pump	—
Valve	Valve2	—
PSA	SEP2	—

Abbreviation: WGS, water gas shift.

ijer, 2024, 1, Downloaded from https://onlinelibrary.wiley.com/doi/10.1155/er/3249514 by Cranfield University Kings, Wiley Online Library on [21/01/2025]. See the Terms and Conditions (https://onlinelibrary.wiley.com/terms-and-conditions) on Wiley Online Library for rules of use; OA articles are governed by the applicable Creative Commons License

TABLE 2: NG specification implemented in the simulation [31].

Parameter	Value
Temperature (°C)	15
Pressure (bar)	1.25
Composition (mol [%])	
Methane	89
Ethane	7
Propane	1
Butane	0.1
Pentane	0.01
CO_2	2
N_2	0.89
Lower heating value (MJ/kg)	46.5

Abbreviation: NG, natural gas.

The mass balance and composition for the main streams of the process are summarised in Table 4.

3. Techno-Economic and Environmental Assessment Indicators

The thermodynamic performance is evaluated by overall energy efficiency (OEE), considering the system's input/output thermal energy and available heat:

$$\mathrm{OEE} = \frac{\dot{m}_{\mathrm{H_2}} \times \mathrm{LHV}_{\mathrm{H_2}} + Q_{Av}}{\dot{m}_{\mathrm{NG}} \times \mathrm{LHV}_{\mathrm{NG}}}, \tag{1}$$

$$\mathrm{CCR}\,(\%) = \frac{\dot{m}_{\mathrm{CO_2,captured}}}{\dot{m}_{\mathrm{CO_2,NG}}}, \tag{2}$$

where $\dot{m}_{\mathrm{H_2}}$, $\dot{m}_{\mathrm{NG}}$ and $\dot{m}_{\mathrm{CO_2}}$ are the mass flow rate of hydrogen, NG and CO_2. In addition, $\mathrm{LHV}_{\mathrm{H_2}}$ and $\mathrm{LHV}_{\mathrm{NG}}$ are respective lower heating values for hydrogen and NG. In addition, Q_{Av} is the available heat emanating from the power generation cycle. Moreover, carbon capture rate (CCR) and cold gas efficiency (CGE) are other thermodynamic performance indicators. CCR quantifies the percentage of CO_2 captured compared to the total CO_2 produced. On the other hand, CGE correlates the thermal energy output and the thermal energy input, as per Equation (3). This metric provides insights into the system's efficiency in converting the input energy from NG into the desired output of the hydrogen stream:

$$\mathrm{CGE} = \frac{\dot{m}_{\mathrm{H_2}} \times \mathrm{LHV}_{\mathrm{H_2}}}{\dot{m}_{\mathrm{NG}} \times \mathrm{LHV}_{G}}. \tag{3}$$

To obtain a better understanding of the economics of the process, the LCOH production (LCOH, €/GJ) and the cost of CO_2 captured (CCC, €/t_{CO_2}) are introduced as the most influential economic factors:

$$\mathrm{LCOH}\left[\frac{€}{\mathrm{GJ}}\right] = \frac{\mathrm{TAC}\left[\frac{M€}{y}\right]}{\dot{m}_{\mathrm{H2}}\left[\frac{kg}{s}\right] \times \mathrm{LHV}_{\mathrm{H2}} \times 3600 \times 8322\left[\frac{h}{y}\right]} \times 1000, \tag{4}$$

$$\mathrm{CCC}\left[\frac{€}{\mathrm{t_{CO2}}}\right] = \frac{\mathrm{TAC}\left[\frac{M€}{y}\right]}{\mathrm{CO_2\ captured}\left[\frac{t}{y}\right]}. \tag{5}$$

The total annualised cost (TAC) is a crucial factor for LCOH calculation, and this parameter is derived from the total plant cost (TPC), the fuel cost (C_{fuel}), the heat revenue (C_{heat}), variable ($V_{\mathrm{O\&M}}$) and fixed ($F_{\mathrm{O\&M}}$) operating and maintenance costs:

$$\mathrm{TAC}\left[\frac{M€}{y}\right] = \mathrm{TPC} \times \mathrm{ACCR} + V_{\mathrm{O\&M}} + F_{\mathrm{O\&M}} + C_{\mathrm{fuel}} + C_{\mathrm{heat}}. \tag{6}$$

The annualised capital charge ratio (ACCR) is a factor that is formulated in Equation (6), considering the project interest rate (r) and project lifetime (n):

$$\mathrm{ACCR} = \frac{r(1+r)^n}{(1+r)^n - 1}. \tag{7}$$

To properly evaluate TAC, Manzolini et al. [34] proposed a model to compute TPC. The equipment purchase cost (C_B) is derived from the reference cost data from the literature and Equation (7), in which C_A, Q_A and f are the reference component cost, capacity and scaling factor, respectively:

$$C_B = C_A\left(\frac{Q_B}{Q_A}\right)^f. \tag{8}$$

The summation of all the individual equipment purchase costs will result in the total equipment cost (TEC) illustrated in Equation (8). The scaling factor (f), reference component cost (C_A) and capacity factor (CF) (Q_A) of different plant components are presented in Table 5:

$$\mathrm{TEC} = \sum_{i}^{n} C_{B,i}. \tag{9}$$

The total direct purchase cost (TDPC) is the total of TEC and the total installation cost (TIC), as shown in Equation (9):

$$\mathrm{TDPC} = \mathrm{TEC} + \mathrm{TIC}. \tag{10}$$

The TPC is calculated from the summation of TDPC, engineering procurement and construction cost (C_{EPC}), the contingencies cost (C_{CO}) and the owner's cost (C_{OC}), as

ijer, 2024, 1, Downloaded from https://onlinelibrary.wiley.com/doi/10.1155/er/3249514 by Cranfield University Kings, Wiley Online Library on [21/01/2025]. See the Terms and Conditions (https://onlinelibrary.wiley.com/terms-and-conditions) on Wiley Online Library for rules of use; OA articles are governed by the applicable Creative Commons License

Table 3: Assumptions to simulate the NG Pox configurations.

Parameter	Value	Reference
MDEA CO_2 absorption process	—	[32]
MDEA/water content in the lean solvent (wt%)	25/72	—
Solvent/CO_2 ratio (wt% basis)	3/25	—
Steam condition at the reboiler (bar)	6.0	—
Pinch point ΔT in the regenerative heat exchanger (°C)	10.0	—
Heat exchangers	—	[33]
Minimum ΔT gas–gas heat exchanger (°C)	25	—
Minimum ΔT gas–liquid heat exchanger (°C)	10	—
Minimum ΔT liquid–liquid heat exchanger (°C)	10	—
Turbomachines	—	—
Turbine isentropic efficiency (%)	93	—
Turbine delivery pressure (bar)	1.015	—
Pump hydraulic/mech efficiency (%)	75/95	—
CO_2 compression train	—	[33]
Number of stages	2	—
Intercooler's temperature (°C)	40	—
Intercooler's pressure drops (P_{inlet} [%])	5	—
Isentropic efficiency (%)	89	—
Mechanical efficiency (%)	95	—
CO_2 delivery pressure (bar)	110	—
CO_2 delivery temperature (°C)	25	—

Abbreviations: MDEA, methyl diethanolamine; NG, natural gas; POx, partial oxidation.

Table 4: Mass flow, temperature, pressure, and composition of the main streams.

Streams	6	8	10	7	14	11	18	20	25	26	27	28
P (bar)	20	20	20	20	20	20	3	2.9	2.9	2.5	1.0	110
T (°C)	300	950	950	300	129	1,200	300	205	39.4	51.9	25	26
m (kg/s)	17	27	24	2.6	27.3	32.9	31.3	31.3	30.3	6.4	2.1	24.5
Composition												
H_2O	—	21.1	21.1	—	0.9	15.3	37.4	20.6	2.0	4.7	—	2.6
O_2	95	—	—	95	5.9	5.0	—	—	0.2	0.3	—	—
Ar	4.0	1.2	1.2	4.0	7.1	6.0	0.9	0.9	1.3	1.9	—	—
N_2	1.0	0.5	0.5	1.0	2.3	1.9	0.4	0.4	0.6	0.8	—	—
CO	—	31.4	31.4	—	—	—	24.9	8.2	1.9	2.3	—	—
CO_2	—	2.7	2.7	—	83.7	71.5	2.1	18.9	31.2	1.4	—	97.2
H_2	—	42.9	42.9	—	—	—	34.0	50.8	62.4	88.4	~1	—

Table 5: Scaling parameters for the component purchase cost.

Component	Scaling factor	C_A (M€)	Q_A	f	Reference
CO_2 capture unit (MDEA)	CO_2 mass flow rate (t/h)	8.8	12.4	0.6	[35]
CO_2 purification unit	Mass flow (t/h)	55.98	266.6	0.6	[35]
CO_2 compressor and condenser	Power (MW)	44	50.5	0.67	[34]
Compressor	Power (kW)	0.44	413	0.68	[35]
WGS	H_2 and CO flow rate (kmol/s)	18.34	2.45	0.65	[36]
Fuel compressor	Power (MW)	8.1	15.3	0.67	[34]
Gas turbine	Power (MW)	49.4	272.1	0.67	[34]
Heat exchanger	Heat transfer (MW)	6.1	828	0.67	[34]
Air separation unit	Oxygen flow rate (kg/s)	26.6	28.9	0.7	[37]
PSA unit	Flow rate (kmol/h)	34.3	17,000	0.6	[38]

Abbreviations: MDEA, methyl diethanolamine; WGS, water gas shift.

ijer, 2024, 1, Downloaded from https://onlinelibrary.wiley.com/doi/10.1155/er/3249514 by Cranfield University Kings, Wiley Online Library on [21/01/2025]. See the Terms and Conditions (https://onlinelibrary.wiley.com/terms-and-conditions) on Wiley Online Library for rules of use; OA articles are governed by the applicable Creative Commons License

Table 6: Assumptions for the economic analysis.

Parameter	Value	Reference
Installation cost as a fraction of total purchase cost (%)	80	[39]
VOM as a fraction of total capital cost (%)	2.0	[40]
FOM as a fraction of total capital cost (%)	1.0	[40]
Plant lifetime (T) (years)	30	[41]
Project interest rate (r) (%)	12	[40]
CF (%)	95	[27]

Abbreviations: CF, capacity factor; FOM, fixed operating cost; VOM, variable operating cost.

Table 7: Life cycle inventory data for the hydrogen production via the POx-CCS system.

Data	Unit	Value
Natural gas	kg/kg_{H2}	4.76
MDEA (make-up)	g/kg_{H2}	3.8
Deionised water	l/kg_{H2}	3.5
Wastewater (condensate)	l/kg_{H2}	0.5
Heat (co-product)	MJ/kg_{H2}	37
CO_2 emissions to air	kg/kg_{H2}	1.13
CO_2 captured for storage	kg/kg_{H2}	11.48

Abbreviations: CCS, carbon capture and storage; MDEA, methyl diethanolamine; POx, partial oxidation.

demonstrated in Equation (10). The C_{EPC} is equal to 15% of the TDPC and the C_{CO} and the C_{OC} are, respectively, 10% and 5% of the TDPC and C_{EPC} summation:

$$TPC = TDPC + C_{EPC} + C_{CO} + C_{OC}. \quad (11)$$

Assumptions for the calculation of the TAC are illustrated in Table 6.

The net climate change impact associated with the hydrogen production from NG POx integrated with CCS is assessed as per the ISO 14040/44 standards [42, 43] for the LCA. The scope of the study is from cradle to gate and includes the construction of the POx plant, the production of NG, the production of hydrogen and heat in the POx plant, the MDEA CO_2 absorption process and the compression of captured CO_2. The unit of analysis is defined as the 'production of 1 kg of hydrogen'. It is assumed that the plant is in the United Kingdom. The key inventory data are provided in Table 7. The construction-related impacts are estimated using LCA data from Ecoinvent v3.8 [44] for various plant equipment. The LCA data for NG, deionised water and waste disposal are also obtained from Ecoinvent [44] v3.8. Since the Ecoinvent v3.8 database does not have the data for MDEA, they are estimated using a stoichiometric relation and the data for methylamine and ethylene oxide from Ecoinvent. The impact allocation between hydrogen and heat (co-product) is carried out using energy allocation.

4. Results and Discussion

The technical performance of the plant is presented in Table 8. It reveals that the proposed system's hydrogen production rate is 2.1 kg/s while the MDEA unit captures 91% of the produced CO_2. The system is designed to be stand-alone. The power requirement for ASU and compression is internally generated for the utilities within the plant by the expander and gas turbine. The expander and gas turbine (both with a pressure ratio of 6.6) generate 23 MW and 15.6 MW of power, respectively. The ASU, with a 15.2 MW power requirement, is the highest power consumption component of the system. The heat for the steam generation required in the WGS process is provided by cooling down the WGS outlet stream. The heat requirement for the reboiler is 27.1 MW, which results in 1.1 MJ/kg_{CO2} specific heat requirement and is generated internally by cooling down the exhaust gas from expander and gas turbine. The remaining technical and thermodynamic performance data of this POx system are summarised in Table 8.

The economic aspect of this plant is presented in Table 9. It can be seen that the carbon capture and compression units are responsible for over 36% of the TEC. The TDPC is calculated to be €232 M. Putting the annual investment under scrutiny, it is found that the plant imposes a yearly cost of €124.2M. However, considering the revenue of heat production, it can be seen that this would compensate for an amount of 7.3 M€/year and reduces the TAC value to a net amount of 116.9 M€/year.

The TAC depends on the energy cost. But, the impact of the energy price on the TAC varies along the project's lifetime. Therefore, the energy price is expressed as the equivalent averaged energy price:

$$C_{eq} = \frac{\sum_{i=1}^{N} \frac{C_i}{(1+r)^i}}{\sum_{i=1}^{N} \frac{1}{(1+r)^i}}, \quad (12)$$

where C_{eq} and C_i represent the equivalent and annual energy for the lifetime N. The C_{eq} for the different discount rates is presented in Table 10.

ijer, 2024, 1, Downloaded from https://onlinelibrary.wiley.com/doi/10.1155/er/3249514 by Cranfield University Kings, Wiley Online Library on [21/01/2025]. See the Terms and Conditions (https://onlinelibrary.wiley.com/terms-and-conditions) on Wiley Online Library for rules of use; OA articles are governed by the applicable Creative Commons License

Table 8: Thermodynamic performance summary of the POx system.

Parameters	Unit	Value	
		Without CCS	With CCS
NG flow rate	kg/s	10	10
Thermal input	MW_{th}	465	465
Gas turbine power generation	MW_e	10.3	23.1
Syngas expander power generation	MW_e	19.6	17.7
NG compression power consumption	MW_e	4.5	4.5
ASU power consumption	MW_e	15.2	15.2
Oxygen compression power consumption	MW_e	7.2	7.2
CO_2 compression power consumption	MW_e	—	7.1
Recycled gas compressor power consumption	MW_e	3.0	6.8
Heat requirement for the reboiler	MW_{th}	—	27.1
Net heat available	MW_{th}	97.6	77.8
CO_2 emission	kg/s	24.8	0.9
CO_2 flow rate for storage	kg/s	—	23.9
Carbon capture rate	%	—	96.4
H_2 production rate/purity	(Kg/s)/(%)	2.3/99.9	2.1/99.9
Thermal output	MW_{th}	285.9	261.1
Cold gas efficiency	%	61.5	56
Overall energy efficiency	%	82.5	73

Abbreviations: ASU, air separation unit; NG, natural gas; POx, partial oxidation.

Table 9: Economic performance summary of the Pox-CCS system.

Parameter	Unit	Value
MDEA unit	M€	29.0
WGS reactors + heat exchanger	M€	22.9
Gas turbine(s)	M€	16.7
CO_2 compressor units	M€	17.7
PSA	M€	15.7
NG compressor	M€	3.6
ASU + O_2 compressor	M€	22.5
Total equipment cost (TEC)	M€	128.9
Total installation cost (TIC)	M€	103.1
Total direct plant cost (TDPC)	M€	232.0
Total plant cost (TPC)	M€	336.4
Annualised plant cost	M€/year	34.7
Fuel cost[a]	M€/year	79.4
Heat revenue[b]	M€/year	7.3
Fixed O&M	M€/year	6.7
Variable O&M	M€/year	3.4
Total annualised cost	M€/year	116.9
LCOH	€/kg_{H2}	1.8
CO_2 capture cost	€/t_{CO2}	160.9

Abbreviations: ASU, air separation unit; CCS, carbon capture and storage; LCOH, levelised cost of hydrogen; Pox, partial oxidation; TDPC, total direct plant cost; TEC, total equipment cost; TIC, total installation cost; TPC, total plant cost.
[a]NG price for the initial economic results is €5.7/GJ.
[b]Heat price for the economic assessment is assumed to be 55% of the NG price.

Figure 2 illustrates the impact of interest rate on the LCOH and the cost of CO_2 capture. Although increasing the discount rate from 3.5% to 12% decreases the energy (fuel and heat) price, it increases the annual capital cost from 12.2 M€ to 41.6 M€; and consequently, the LCOH (from 1.5 €/kg_{H2} to 1.9 €/kg_{H2}) and cost of CO_2 capture (from 134.2 €/t_{CO2} to 168.0 €/t_{CO2}).

The effect of fuel price on the LCOH and the cost of CO_2 capture is illustrated in Figure 3. It is worth mentioning that the heat price correlation with the fuel price is still kept

ijer, 2024, 1, Downloaded from https://onlinelibrary.wiley.com/doi/10.1155/er/3249514 by Cranfield University Kings, Wiley Online Library on [21/01/2025]. See the Terms and Conditions (https://onlinelibrary.wiley.com/terms-and-conditions) on Wiley Online Library for rules of use; OA articles are governed by the applicable Creative Commons License

Table 10: Equivalent energy cost dependence on the discount rate.

Discount rate (%)	NG price (€/GJ)	Heat price (€/GJ)
3.5	5.9	3.2
10	5.7	3.1
12	5.5	3.0

Abbreviation: NG, natural gas.

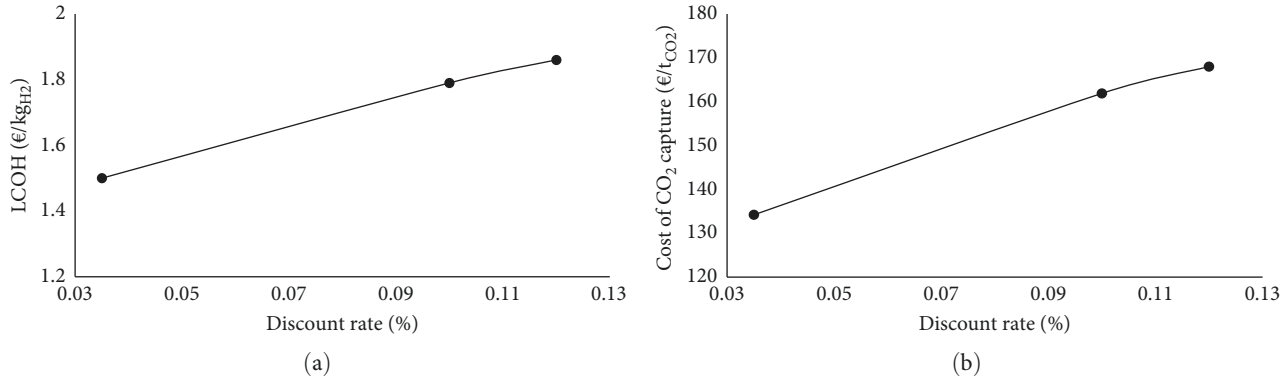

Figure 2: The effect of interest rate on LCOH (a) and cost of CO_2 capture (b). LCOH, levelised cost of hydrogen.

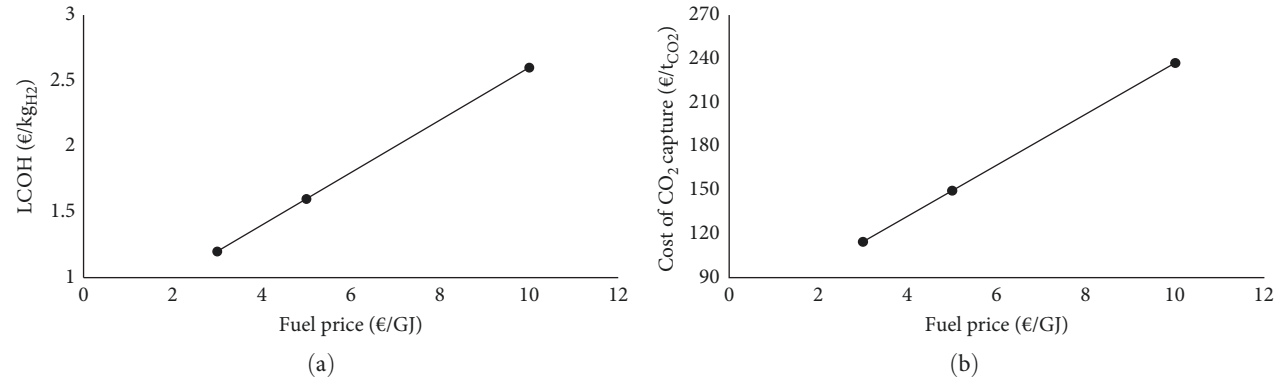

Figure 3: Effect of fuel price on LCOH (a) and cost of CO_2 capture (b). LCOH, levelised cost of hydrogen.

constant in this sensitivity analysis. Therefore, while the fuel price ranges between 3 and 10 €/GJ, the heat price ranges between 1.6 and 5.5 €/GJ simultaneously. Figure 3 reveals a direct correlation between the fuel price and LCOH and the cost of CO_2 capture. At the fuel price of 3 €/GJ, the LCOH and capture costs are 1.2 €/kg_{H2} and 114.6 €/t_{CO2}, respectively. However, an increment of the fuel price by 7 €/GJ raises the LCOH and the capture costs to 2.6 €/kg_{H2} and 237.2 €/t_{CO2}.

It is worth mentioning that considering a wide range of fuel prices and discount rates offers a sufficient understanding of the LCOH in various scenarios.

As shown in Figure 4, the climate change impact of hydrogen production via the POx with and without the CCS system is 1.1 $kg_{CO2\ eq.}$/kg_{H2} and 8.6 $kg_{CO2\ eq.}$/kg_{H2}, respectively. For the POx-CCS system, using NG accounts for 69%, while the CO_2 emissions from the process contribute to 30%. On the other hand, the contributions of plant construction, MDEA and waste disposal are very small (<1%). In the case of POx without the CCS system, the climate change impact is mainly due to CO_2 emissions from the POx system, which accounts for 92% of the impact, while the contribution of NG is 7.7%. Therefore, the climate change impact of hydrogen production via the POx with and without CCS processes is 69% and 25% lower than those of the SMR with CCS and SMR without CCS processes, respectively. Pox's lower climate change impact than SMR is mainly due to the exothermic nature of POx and combustion, which eliminates the need for external heat, significantly reducing CO_2 emissions. Moreover, the excess heat within the system can be utilised elsewhere to eliminate the associated CO_2 emission for heat production.

SMR is still the leading hydrogen production technology with an LCOH of about 1 €/kg_{H2} for SMR without CCS and 1.5 €/kg_{H2} with CCS integration [45]. Coal gasification with CCS, while more expensive, has an LCOH of 2.8 €/kg_{H2} [45], reflecting the higher costs associated with capturing and storing carbon from coal. Electrolysis using grid electricity remains costly at 3.0–6 €/kg_{H2} without CCS, but when powered by renewable energy, the LCOH can be competitive,

ijer, 2024, 1, Downloaded from https://onlinelibrary.wiley.com/doi/10.1155/er/3249514 by Cranfield University Kings, Wiley Online Library on [21/01/2025]. See the Terms and Conditions (https://onlinelibrary.wiley.com/terms-and-conditions) on Wiley Online Library for rules of use; OA articles are governed by the applicable Creative Commons License

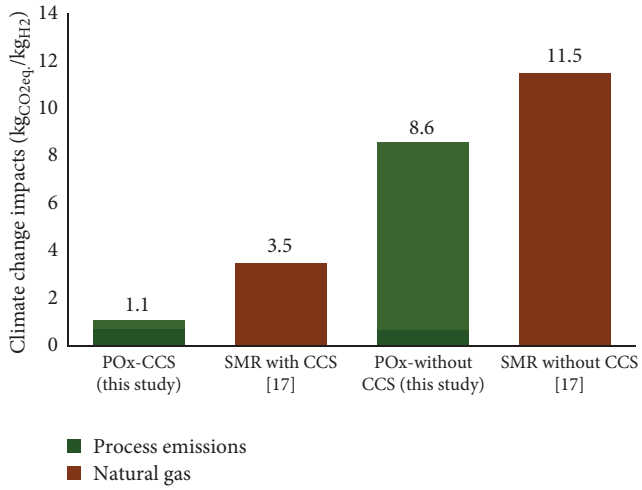

FIGURE 4: Climate change impact of H_2 production via the POx system and comparison with the SMR process. CCS, carbon capture and storage; POx, partial oxidation; SMR, steam methane reforming.

around 1.7–3.7 €/kg_{H2}, depending on electricity prices and electrolyser efficiencies [46].

When considering cradle-to-gate analysis, the environmental impact of hydrogen production methods varies significantly in terms of carbon emissions. SMR with CCS can reduce emissions to about 1–3 $kg_{CO2\ eq.}/kg_{H2}$ [47], significantly lower than the 11 $kg_{CO2\ eq.}/kg_{H2}$ without CCS [48]. Coal gasification with CCS, though still carbon-intensive, reduces emissions to ~5–10 $kg_{CO2\ eq.}/kg_{H2}$ compared to the 18–20 kg $kg_{CO2\ eq.}/kg_{H2}$ without CCS [49]. Electrolysis using grid electricity remains relatively high at 11.1 $kg_{CO2\ eq.}/kg_{H2}$ without CCS [48], but when paired with renewable energy, it has a carbon footprint close to zero, about 0–1 $kg_{CO2\ eq.}/kg_{H2}$ [48]. It is found that the proposed cycle, with a 96.4% CO_2 capture rate, a climate change impact of 1.1 $kg_{CO2\ eq.}/kg_{H2}$, and an LCOH ranging from 1.2 €/kg_{H2} to 2.6 €/kg_{H2} (at different interest rates and fuel prices), is competitive with state-of-the-art hydrogen production technologies.

5. Conclusions

This study investigated a stand-alone system for hydrogen generation that exploits NG as the feedstock. The system is simulated using Aspen Plus software and evaluated from techno-economic and environmental points of view. The system's technical analysis reveals that the plant's overall energy and CGE are 73% and 56%, respectively. Moreover, the heat recovery of 77.8 MW generates a revenue of about 7.3 €/year. A detailed economic assessment reveals that this system, with an LCOH of 1.8 €/kg_{H2}, is competitive with other state-of-the-art hydrogen production technology, such as SMR integrated with CCS. The LCA findings also indicate that the climate change impact of hydrogen production via the POx-CCS process is 69% lower than that of the SMR with the CCS process (1.1 $kg_{CO2\ eq.}/kg_{H2}$ and 3.5 $kg_{CO2\ eq.}/kg_{H2}$, respectively). The system (with 0.9 kg/s CO_2 emission) achieves a CCR of 96%. Additionally, the lower climate change impact of the evaluated system is due to the excess heat of 77.8 MW, which can be utilised for other purposes, compensating for CO_2 emission.

Nomenclature

$\dot{m}$:	Mass flow rate
f:	Scaling factor
$F_{O\&M}$:	Fixed operating and maintenance cost
r:	Interest rate
T:	Project lifetime
$V_{O\&M}$:	Variable operating and maintenance cost
W_{net}:	The net power output of the entire system
η_{th}:	Net thermal efficiency
C_A:	Reference equipment cost
C_B:	Equipment capital cost
Q_A:	Reference equipment capacity
Q_B:	Equipment capacity
η:	Isentropic efficiency.

Abbreviations

ASU:	Air separation unit
CCR:	Carbon capture rate
CCS:	Carbon capture and storage
CF:	Capacity factor
CGE:	Cold gas efficiency
GWP:	Global warming potential
HTR:	High-temperature reactor
LCOH:	Levelised cost of hydrogen
LHV:	Lower heating value
MDEA:	Methyl diethanolamine
NG:	Natural gas
OC:	Owner's cost
SMR:	Steam methane reforming
TAC:	Total annualised cost
TPC:	Total plant cost.

Data Availability Statement

All the relevant data are included in the paper.

Conflicts of Interest

The authors declare no conflicts of interest.

Funding

No funding was received for this manuscript

References

[1] S. Ogo and Y. Sekine, "Recent Progress in Ethanol Steam Reforming Using Non-Noble Transition Metal Catalysts: A Review," *Fuel Processing Technology* 199 (2020): 106238.

[2] W.-H. Chen, T.-W. Chiu, and C.-I. Hung, "Enhancement Effect of Heat Recovery on Hydrogen Production From Catalytic Partial Oxidation of Methane," *International Journal of Hydrogen Energy* 35, no. 14 (2010): 7427–7440.

[3] D. Fraile, J. C. Lanoix, P. Maio, A. Rangel, and A. Torres, "Overview of the Market Segmentation for Hydrogen Across

ijer, 2024, 1, Downloaded from https://onlinelibrary.wiley.com/doi/10.1155/er/3249514 by Cranfield University Kings, Wiley Online Library on [21/01/2025]. See the Terms and Conditions (https://onlinelibrary.wiley.com/terms-and-conditions) on Wiley Online Library for rules of use; OA articles are governed by the applicable Creative Commons License

Potential Customer Groups," *Based on Key Application Areas, European Commission* (2015): 1–32.
[4] M. Binder, M. Kraussler, M. Kuba, and M L, *Hydrogen From Biomass*, 85 (IEA Bioene, 2018).
[5] J. Bilik, P. Pustejovska, S. Brozova, and S. Jursova, "Efficiency of Hydrogen Utilization in Reduction Processes in Ferrous Metallurgy," *Scientia Iranica* 20 (2013): 337–342.
[6] K. Rechberger, A. Spanlang, A. Sasiain Conde, H. Wolfmeir, and C. Harris, "Green Hydrogen-Based Direct Reduction for Low-Carbon Steelmaking," *Steel Research International* 91, no. 11 (2020).
[7] C. Antonini, K. Treyer, A. Streb, Spek M. van der, C. Bauer, and M. Mazzotti, "Hydrogen Production From Natural Gas and Biomethane With Carbon Capture and Storage—A Techno-Environmental Analysis," *Sustainable Energy & Fuels* 4, no. 6 (2020): 2967–2986.
[8] J. Hu, S. Chen, and W. Xiang, "Ni, Co and Cu-promoted Iron-Based Oxygen Carriers in Methane-Fueled Chemical Looping Hydrogen Generation Process," *Fuel Processing Technology* 221 (2021): 106917.
[9] H.F.C.A.UK, "The Case for Blue Hydrogen," in *UK Hydrogen and Fuel Cell Association Position Paper*, (2021): 1–16.
[10] S. Dermühl and U. Riedel, "A Comparison of the Most Promising Low-Carbon Hydrogen Production Technologies," *Fuel* 340 (2023): 127478.
[11] Hydrogen Council, "Path to Hydrogen Competitiveness A Cost Perspective," (2020).
[12] C. Bauer, K. Treyer, C. Antonini, et al., "On the Climate Impacts of Blue Hydrogen," *Sustainable Energy & Fuels* 6, no. 1 (2021): 66–75.
[13] X. Dong, Y. Liu, S. Cheng, H. Zhou, W. Zhang, and B. Jin, "Molten Salt Induced Synthesis of Ni-Sn-Al Ternary Oxide as Highly Efficient Catalyst for Low S/C Ratio Methane Steam Reforming," *Fuel Processing Technology* 247 (2023): 107800.
[14] P. Sun, B. Young, A. Elgowainy, et al., "Criteria Air Pollutants and Greenhouse Gas Emissions From Hydrogen Production in U.S. Steam Methane Reforming Facilities," *Environmental Science & Technology* 53, no. 12 (2019): 7103–7113.
[15] B. Gaudernack and S. Lynum, "Hydrogen From Natural Gas Without Release of CO_2 to the Atmosphere," *International Journal of Hydrogen Energy* 23, no. 12 (1998): 1087–1093.
[16] P. Gangadharan, K. C. Kanchi, and H. H. Lou, "Evaluation of the Economic and Environmental Impact of Combining Dry Reforming With Steam Reforming of Methane," *Chemical Engineering Research and Design* 90, no. 11 (2012): 1956–1968.
[17] Y. Khojasteh Salkuyeh, B. A. Saville, and H. L. MacLean, "Techno-Economic Analysis and Life Cycle Assessment of Hydrogen Production From Natural Gas Using Current and Emerging Technologies," *International Journal of Hydrogen Energy* 42, no. 30 (2017): 18894–18909.
[18] S. Roussanaly, R. Anantharaman, and C. Fu, *Low-Carbon Footprint Hydrogen Production From Natural Gas: A Techno-Economic Analysis of Carbon Capture and Storage From Steam-Methane Reforming* 81 (2020): 1015–1020.
[19] P. Chawdhury, K. V. S. S. Bhargavi, and C. Subrahmanyam, "A Single-Stage Partial Oxidation of Methane to Methanol: A Step Forward in the Synthesis of Oxygenates," *Sustainable Energy & Fuels* 5, no. 13 (2021): 3351–3362.
[20] A. Ugwu, A. Zaabout, F. Donat, et al., "Combined Syngas and Hydrogen Production Using Gas Switching Technology," *Industrial & Engineering Chemistry Research* 60, no. 9 (2021): 3516–3531.
[21] F. Qureshi, M. Yusuf, M. Arham, et al., "A State-of-the-Art Review on the Latest Trends in Hydrogen Production, Storage, and Transportation Techniques," *Fuel* 340 (2023): 127574.
[22] P. H. Pandey, T. M. Ukarde, J. S. Mahale, A. Vasishta, and H. S. Pawar, "Syngas Production via Biomass Gasification," *Biomass, Biofuels, Biochemicals* (2022): 211–261.
[23] H. S. Das, M. F. F. Chowdhury, S. Li, and C. W. Tan, "9. Fuel Cell and Hydrogen Power Plants," *Hybrid Renewable Energy Systems and Microgrids, Academic Press* (2021): 313–349.
[24] C. Wang, M. Liao, B. Liang, et al., "Enhancement Effect of Catalyst Support on Indirect Hydrogen Production From Propane Partial Oxidation Towards Commercial Solid Oxide Fuel Cell (SOFC) Applications," *Applied Energy* 288 (2021): 116362.
[25] Y. Chih, Y. Su, W. Chen, et al., "Optimization for Hydrogen Production From Methanol Partial Oxidation Over Ni-Cu /Al2O3 Catalyst under Sprays," *International Journal of Hydrogen Energy* 47, no. 96 (2022): 40559–40572.
[26] A. A. Levikhin and A. A. Boryaev, "High-Temperature Reactor for Hydrogen Production by Partial Oxidation of Hydrocarbons," *International Journal of Hydrogen Energy* 48, no. 72 (2023): 28187–28204.
[27] Y. Yan, V. Manovic, E. J. Anthony, and P. T. Clough, "Techno-Economic Analysis of Low-Carbon Hydrogen Production by Sorption Enhanced Steam Methane Reforming (SE-SMR) Processes," *Energy Conversion and Management* 226 (2020): 113530.
[28] S. Ghiami, N. Khallaghi, and T. N. Borhani, "Techno-Economic and Environmental Assessment of Staged Oxy-Co-Firing of Biomass-Derived Syngas and Natural Gas," *Energy Conversion and Management* 243 (2021): 114410.
[29] N. Khallaghi, S. Z. Abbas, G. Manzolini, E. De Coninck, and V. Spallina, "Techno-Economic Assessment of Blast Furnace Gas Pre-Combustion Decarbonisation Integrated With the Power Generation," *Energy Conversion and Management* 255 (2022): 115252.
[30] M. C. Romano, P. Chiesa, and G. Lozza, "Pre-Combustion CO_2 Capture From Natural Gas Power Plants, With ATR and MDEA Processes," *International Journal of Greenhouse Gas Control* 4, no. 5 (2010): 785–797.
[31] R. Scaccabarozzi, M. Gatti, and E. Martelli, "Thermodynamic Analysis and Numerical Optimization of the NET Power Oxy-Combustion Cycle," *Applied Energy* 178 (2016): 505–526.
[32] M. Gazzani, M. C. Romano, and G. Manzolini, "CO_2 Capture in Integrated Steelworks by Commercial-Ready Technologies and SEWGS Process," *International Journal of Greenhouse Gas Control* 41 (2015): 249–267.
[33] V. Spallina, P. Nocerino, M. C. Romano, M. van Sint Annaland, S. Campanari, and F. Gallucci, "Integration of Solid Oxide Fuel Cell (SOFC) and Chemical Looping Combustion (CLC) for Ultra-High Efficiency Power Generation and CO_2 Production," *International Journal of Greenhouse Gas Control* 71 (2018): 9–19.
[34] G. Manzolini, A. Giuffrida, P. D. Cobden, H. A. J. van Dijk, F. Ruggeri, and F. Consonni, "Techno-Economic Assessment of SEWGS Technology When Applied to Integrated Steel-Plant for CO_2 Emission Mitigation," *International Journal of Greenhouse Gas Control* 94 (2020): 102935.
[35] A. M. Cormos, I. Dumbrava, and C. C. Cormos, "Evaluation of Techno-Economic Performance for Decarbonized Hydrogen and Power Generation Based on Glycerol Thermo-Chemical Looping Cycles," *Applied Thermal Engineering* 179 (2020): 115728.
[36] G. Zang, J. Jia, S. Tejasvi, A. Ratner, and E. Silva Lora, "Techno-Economic Comparative Analysis of Biomass

ijer, 2024, 1, Downloaded from https://onlinelibrary.wiley.com/doi/10.1155/er/3249514 by Cranfield University Kings, Wiley Online Library on [21/01/2025]. See the Terms and Conditions (https://onlinelibrary.wiley.com/terms-and-conditions) on Wiley Online Library for rules of use; OA articles are governed by the applicable Creative Commons License

Integrated Gasification Combined Cycles With and Without CO_2 Capture," *International Journal of Greenhouse Gas Control* 78 (2018): 73–84.
[37] S. Campanari, P. Chiesa, G. Manzolini, and S. Bedogni, "Economic Analysis of CO_2 Capture From Natural Gas Combined Cycles Using Molten Carbonate Fuel Cells," *Applied Energy* 130 (2014): 562–573.
[38] DOE/NETL, "Assessment of Hydrogen Production with CO_2 Capture Volume 1: Baseline State-of- the-Art Plants," (2010).
[39] V. Stenberg, V. Spallina, T. Mattisson, and M. Rydén, "Techno-Economic Analysis of H2 Production Processes Using Fluidized Bed Heat Exchangers With Steam Reforming—Part 1: Oxygen Carrier Aided Combustion," *International Journal of Hydrogen Energy* 45, no. 11 (2020): 6059–6081.
[40] D. P. Hanak, B. G. Jenkins, T. Kruger, and V. Manovic, "High-Efficiency Negative-Carbon Emission Power Generation From Integrated Solid-Oxide Fuel Cell and Calciner," *Applied Energy* 205 (2017): 1189–1201.
[41] N. Khallaghi, D. P. Hanak, and V. Manovic, "Staged Oxy-Fuel Natural Gas Combined Cycle," *Applied Thermal Engineering* 153 (2019): 761–767.
[42] ISO, "Environmental Management - Life Cycle Assessment - Principles and Framework (ISO 14040: 2006), Geneva, Switzerland," (2006).
[43] ISO, "ISO 14044: Environmental Management - Life Cycle Assessment - Requirements and Guidelines. Geneva, Switzerland:" (2006).
[44] Ecoinvent, "Ecoinvent v3.7 Database. Dübendorf, Switzerland: Swiss Centre for Life Cycle Inventories:" (2020).
[45] NETL, "Comparison of Commercial, State-of-the-Art, Fossil-Based Hydrogen Production Technologies," (2022).
[46] IEA, "The Future of Hydrogen," (2019).
[47] IEA, "Low-Carbon Hydrogen from Natural Gas: Global Roadmap," (2022).
[48] Hydrogen Council, "Hydrogen Decarbonization Pathways A Life-Cycle Assessment," (2021).
[49] T. Koch Blank and P. Molly, "Hydrogen's Decarbonization Impact for Industry Near-Term Challenges and Long-Term Potential," (2020).

ijer, 2024, 1, Downloaded from https://onlinelibrary.wiley.com/doi/10.1155/er/3249514 by Cranfield University Kings, Wiley Online Library on [21/01/2025]. See the Terms and Conditions (https://onlinelibrary.wiley.com/terms-and-conditions) on Wiley Online Library for rules of use; OA articles are governed by the applicable Creative Commons License

https://dspace.org/

Blue hydrogen production through partial oxidation: a technoeconomic and life cycle assessment

Khallaghi, Navid; Ghiami, Shamsoddin; Jeswani, Harish; Nabavi, Seyed Ali; Anthony, Edward J.

Klyamkin, Semen

2024

Wiley

https://doi.org/10.1155/er/3249514

Khallaghi N, Ghiami S, Jeswani H, et al., (2024) Blue hydrogen production through partial oxidation: a technoeconomic and life cycle assessment. International Journal of Energy Research, Volume 2024, December 2024, Article number 3249514

Downloaded from a DSpace repository. https://dspace.org/